M4E.001

R. Liu, J. N. Nilchi, Y. Lin, T. L. Naing, and C. T.-C. Nguyen, "Zero quiescent power VLF mechanical communication receiver," *Proceedings* of the 18th Int. Conf. on Solid-State Sensors, Actuators, & Microsystems (Transducers'15), Anchorage, Alaska, June 21-25, 2015, pp. 129-132.

ZERO QUIESCENT POWER VLF MECHANICAL COMMUNICATION RECEIVER

R. Liu, J. Naghsh Nilchi, Y. Lin, T.L. Naing, and C.T.-C. Nguyen
University of California, Berkeley, USA

ABSTRACT

A first-in-kind all-mechanical communication receiver front-end employing resonant micromechanical switch (i.e., resoswitch) technology has detected and demodulated frequency shift keyed (FSK) signals as low as −60dBm at a VLF frequency of 20kHz suitable for extremely long-range communications, all while consuming zero quiescent power when in standby. The key to attaining high quality signal reception and demodulation with zero quiescent power consumption derives from the use of heavily nonlinear amplification, provided by mechanical impact switching of the resoswitch. This approach would be inconceivable in a conventional receiver due to performance degradation caused by nonlinearity, but becomes plausible here by virtue of the RF channel-selection provided by the resonant behavior of the mechanical circuit.

KEYWORDS

RF MEMS switch, resonant switch, FSK, receiver front end, RF channel selection, nonlinear amplifier.

INTRODUCTION

Very Low Frequency (VLF) and Low Frequency (LF) receivers operating from 3-30 and 30-300 kHz, respectively, with wavelengths on the order of kilometers, present a compelling opportunity for very long-range communications, such as depicted in Figure 1. In particular, while high frequency radio waves propagate omnidirectionally along line of sight paths, so suffer from free space path losses proportional to the square of the distance between transmitter and receiver; VLF and LF signals propagate by surface wave through an effective waveguide formed by the ionosphere and the earth that confines their energy to follow the curvature of the earth, and hence, suffer less loss [1]. Such frequencies are presently used for time transfer over long distances, where their propagation by ground wave eliminates multipath issues, ultimately helping to maintain timing precision. Smaller, zero quiescent power versions of such receivers would expand the application set to sensors and other autonomous devices that could be commanded or interrogated from hundreds of miles away.

Unfortunately, operation at such low frequency generally entails the use of large electronic components. In addition, conventional linear approaches to receiver design fall well short of zero quiescent power. A nonlinear approach that could dispense with the power needed to maintain linearity would fare much better. Recognizing this, the approach taken here first harnesses the much smaller acoustic wavelengths of mechanics to allow substantially smaller size than electronic counterparts; and second, dares to employ a very nonlinear mechanical amplifier that becomes key to zero standby power. Use of this approach yields a first-in-kind all-mechanical communication receiver front-end, shown in Figure 2, employing a resonant micromechanical switch (i.e., resoswitch) [2] that detects and demodulates frequency shift keyed (FSK) signals as low as −60dBm at a VLF frequency of 20kHz suitable for extremely long-range communications, all while consuming zero quiescent power when in standby.

Figure 1: VLF and LF communication is possible over thousands of miles, practically crossing continents.

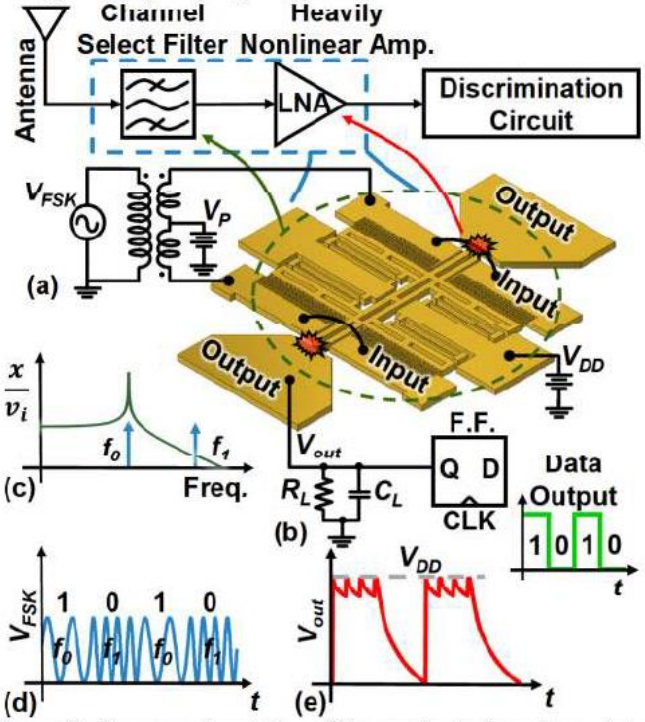

Figure 2: Summary description of the mechanical receiver. (a) A resoswitch serves as a combined channel-select filter with response in (c) and nonlinear amplifier feeding load (b) while consuming zero quiescent power. A (d) FSK input signal generates the output in (e), which in turn produces the bit stream (green) at the flip-flop output.

RECEIVER STRUCTURE AND OPERATION

Figure 2 summarizes the overall receiver structure and operation, where practically all of the front-end functionality relies on a single micromechanical resonant switch (a.k.a.

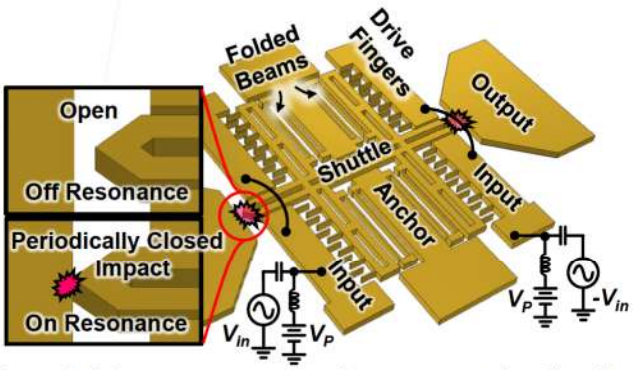

Figure 3: Schematic zooming in on the impact point for off- and on-resonance inputs.

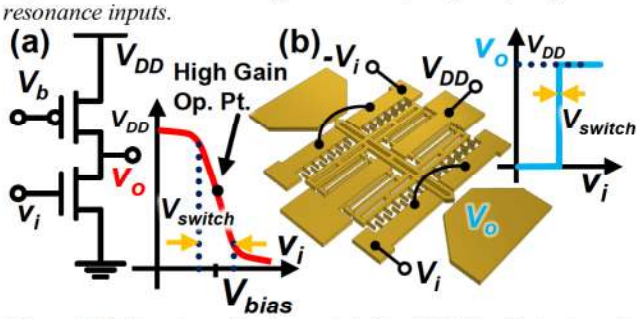

Figure 4: Voltage transfer characteristics (VTC's) of (a) a transistor amplifier; and (b) the resoswitch.

resoswitch) [2], shown more clearly in Figure 3. As shown, the low frequency resoswitch used here comprises a folded-beam-supported comb-driven resonator with a pair of output electrode impacting points at both sides of the shuttle. Four pairs of 60μm-long folded beams suspend the resonator shuttle from central anchor points. To suppress squegging [3], this resoswitch differs from previous ones in its use of fully differential input comb electrodes and impact points, both of which help to overcome impact-induced energy loss. If the differential ac input signal shown is off-resonance, the resoswitch does not move enough to overcome the air gap of d_0 separating the shuttle impact points from the output electrodes, so is electrically open. When the input signal is on or near resonance and has sufficient amplitude, the shuttle vibrates with a large enough amplitude to periodically impact the output electrodes, effectively closing the shuttle-to-output switch at the in-channel signal frequency.

Resoswitch Filter-LNA

The described resonant switching behavior allows the resoswitch to effectively function as a "filter-LNA", such as shown in Figure 2(a). This of course is a series of functions needed in any receiver front-end, but in this case realized via a single device with a heavily nonlinear impact-based amplifier that outright enables zero quiescent power operation.

To see how, consider that the simplest receiver front-end consists of merely an amplifier immediately following the sensor, e.g., an antenna. If the amplifier is a transistor amplifier, then the finite threshold voltage and subthreshold slope of its transistor switching device precludes on/off switched operation, since the microvolt level inputs typically received

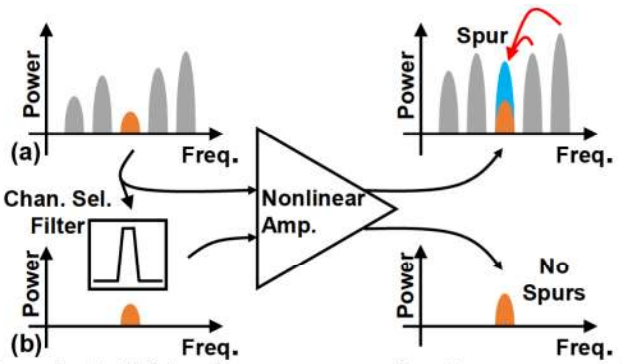

Figure 5: (a) With interferers present, nonlinearity generates spurious signals from those interferers that can mask the desired signal. (b) Removal of all interferers via a channel-select filter removes the source of the spurs, allowing subsequent nonlinearity with little consequence.

are not large enough to induce switching over sub-millisecond integration times. Rather, the transistor must be biased at a high gain operating point, where significant dc current flows, hence, significant power consumption ensues, as shown in Figure 4.

On the other hand, a conventional aperiodic MEMS switch's on/off switching slope is nearly infinite. Unfortunately, its threshold voltage is even larger than that of a transistor, with values ranging from 6V for NEMS logic switches [4] to 85V for RF MEMS switches [5].

The resoswitch used here solves both problems, with not only an effectively infinite on/off slope similar to the aperiodic switch, but also an ability to switch with very low power inputs enabled by Q multiplication of its displacement at resonance. The impulsive contact force of resonance impacting operation also improves contact resistance and reliability, making possible measured cycle counts greater than 170 trillion [2], which is several orders higher than aperiodic counterparts. The constraint to resonant or periodic inputs is actually not a constraint at all for an RF front-end application, and is in fact a benefit when one considers the well-known pitfalls of nonlinear signal processing, especially for receivers.

Indeed, conventional receivers attempt to avoid nonlinearity as much as possible, since nonlinearity generates spurious signals from interfering signals that can mask the desired signal, as shown in Figure 5. The power consumption of a receiver in fact derives in large part from a need to keep the front-end linear, where higher linearity requires more power. But raising power consumption is not the best way to combat nonlinearity. Rather, a much better approach is to eliminate interferers before they experience nonlinearity and generate spurs, as explained in [4] and shown in Figure 5. No interferers, no spurs. Herein lies the beauty of the resoswitch: Its frequency response essentially functions as a built-in channel-selector that filters out all interferers, thereby eliminating nonlinear spurs and enabling its own heavily nonlinear, zero-quiescent power, impact-switching amplifier!

Practical Receiver Operation

As shown in Figure 2(a), the receiver takes as input a

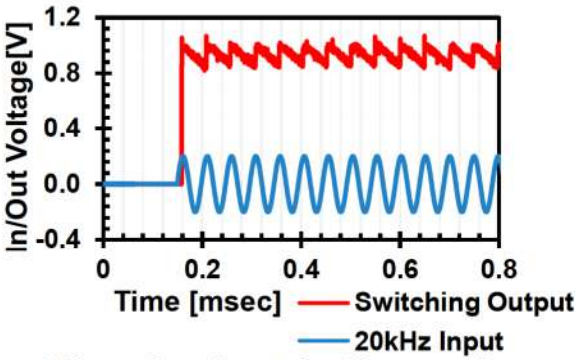

Figure 6: Measured time domain plot of the resoswitch output in response to a 20-kHz on-resonance input that induces impacting, connecting V_{DD} to the output and allowing it to deliver power.

differential ac signal $\pm(1/2)V_{FSK}$ combined with a dc bias voltage V_P applied to resoswitch comb electrodes on opposite sides. A dc voltage source V_{DD} tied to the shuttle as shown in Figure 2(a) serves as the supply to be switched to the output upon impact with the switch electrodes.

When the frequency of V_{FSK} is within the frequency passband of the resoswitch, the shuttle vibrates laterally with an amplitude approximately Q times larger than would ensue with an out-of-band input. If V_{FSK} induces a shuttle displacement larger than the switch gap d_0, the shuttle periodically connects the output to V_{DD} and delivers power to output load R_L and C_L. Figure 6 shows measured input and switch output waveforms for R_L=160kΩ and C_L=100pF. In the receiver schematic of Figure 2(a), a flip-flop following the *RC* circuit then latches the output to provide a more stable sequence of 1's and 0's to the next stage.

The minimum input power that drives the shuttle to displace d_0 governs the ultimate sensitivity of the receiver, which takes the form

$$S = \frac{d_0^2 k_m \omega_0}{Q} \qquad (3)$$

where k_m is the dynamic stiffness of the resoswitch at the shuttle location [7]. Clearly, the smaller the switch gap spacing and higher the Q, the better the sensitivity.

FABRICATION

Figure 7 describes the process flow used to fabricate the resoswitch. The process begins with deposition of 2μm sacrificial LPCVD oxide atop a starting silicon substrate. A seed layer comprised of 7nm Cr/20nm Au/20nm Cr is then evaporated. The bottom layer of Cr serves as an adhesion layer, while the top Cr protects Au during subsequent etching. Next, 3μm of PECVD oxide is deposited as mold material for electroplating, followed by photolithography and etching to define the mold in (b). Use of this oxide mold allows higher resolution i.e., smaller gaps, compared to conventional photoresist molds, which helps sensitivity per (3). This process achieved 800nm gaps between comb fingers, to be compared with the 1.5μm of a previous PR-based mold process [8].

After a short wet dip in Cr etchant Cr-7 to remove the top protection Cr layer, electroplating in a sodium gold sulfite solution forms resoswitch structures over exposed regions of

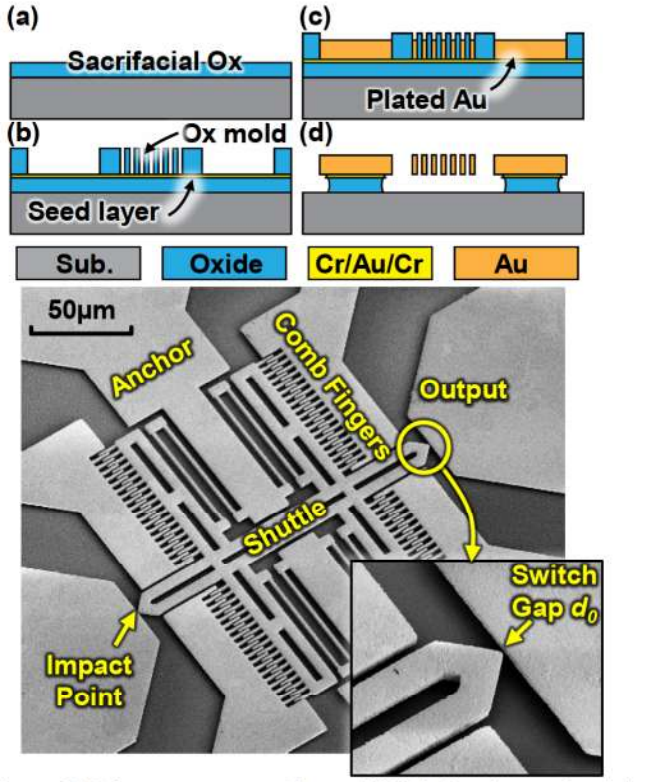

Figure 7: Fabrication process flow and SEM of an electroplated Au comb-driven resoswitch.

Au seed layer. Next, a short dip in hydrofluoric acid (HF) followed by Cr-7 and Au TFA etchants removes the oxide mold and the metal seed layers. Finally, a timed etch in HF releases the structure while preserving sacrificial oxide under the large area anchors. Figure 7 presents the SEM of a released Au resoswitch with a zoom-in on the switch impact point.

EXPERIMENTAL RESULTS

A Lakeshore FWPX vacuum probe station provided the 1mTorr pressure and low-capacitance probes needed to evaluate receiver performance. A Tektronix AFG3200 signal generator provided modulated inputs, while the *RC* and flip-flop demodulation stages were realized on a pc board.

FSK Signal Demodulation

Figure 8 plots the signal waveforms at different points in the receive chain. As shown, the input of Figure 8(a) comprises an FSK modulated random series of data bits "0" and "1", where bit "0" denotes an off resonance frequency at 50kHz and "1" denotes a resonance input at 20kHz. This signal passes through a balun to generate differential inputs that combine with a dc bias V_P of 16V then proceed to resoswitch comb electrodes on opposite sides. A "1" input with sufficient amplitude drives the resoswitch to resonance impacting, which then drives the output to V_{DD} = 1V. Input powers as low as −60dBm were sufficient to incite impacting at the output node, which then delivered −11dBm to the backend circuit. This equates to more than 49dB of power gain, all generated via a mechanical switching mechanism.

On the other hand, an off-resonance "0" input barely

moves the resoswitch shuttle. There is no impact, so the output sinks to ground via bleed resistor R_L. As advertised, the receiver front-end consumes no power when receiving out-of-channel inputs.

Since a true FSK receiver detects both 1's and 0's, the present receiver that explicitly detects only 1's is actually operating in an on/off key (OOK) fashion. Addition of a second resoswitch that specifically detects 0's, so that both 1's and 0's are detected and processed, is all that is needed to make a true FSK receiver.

The RC circuit ultimately governs the bit rate f_b of the present receiver, where proper operation ensues when

$$\frac{1}{2\pi f_0} < R_L C_L < \frac{1}{2\pi f_b} \qquad (2)$$

When R_L and C_L take on values of 160kΩ and 100pF, respectively, Figure 8(b) indicates that the output easily keeps up with a 1kbit/s input bit rate. Note, however, how the output vacillates somewhat at the beginning of each "0" to "1" transition, perhaps indicating squegging-related instability even with the new resoswitch design. Elimination of this phenomenon awaits further investigation.

In the meantime, the receiver of Figure 2(a) simply suppresses output instability by latching to a flip-flop that then presents the stable output shown in Figure 8(c). In this scheme, the first valid "1" is used as a pilot to start the synchronizing clock needed for latching.

Frequency Mask

Figure 9 plots the minimum input power required to instigate reliable impacting, and thus, produce an output, at various input frequencies. The transition from in-channel to out-of-channel is impressively abrupt and quite suitable for high density packing of adjacent channels. Due to an impedance mismatch between the device input and the 50Ω signal generator, the largest available off-resonance signal power for testing was -14dBm. As shown, out-of-channel inputs with this power did not induce output switching, so were rejected. Theory further predicts that 0dBm signals, if they were available, would also be rejected.

It should be noted that LF receivers commonly post input impedances on the order of 40kΩ [9], which match well to magnetic loop near-field antennas. This value is within the range of comb-driven resonator devices with sufficient bias voltage and small finger-to-finger gap spacing [10].

CONCLUSIONS

The demonstrated all-mechanical OOK receiver front-end that detects and demodulates a 20kHz FSK signal at −60dBm, while consuming zero quiescent power, poses some very interesting application possibilities, especially when one recognizes the importance of low power consumption for future sensors to be used in the internet of things. The zero quiescent power consumption of the demonstrated receiver is especially interesting for applications that must "listen" continuously. Perhaps, even more compelling is the actual demonstration via this work of a receiver that embraces hard impacting nonlinearity to reduce power consumption, while alleviating detriments via channel-selection. The sensitivity and frequency range of the present work are conservative, but versions capable of -100dBm sensitivity and operation past VHF are conceivable and the subject of ongoing research.

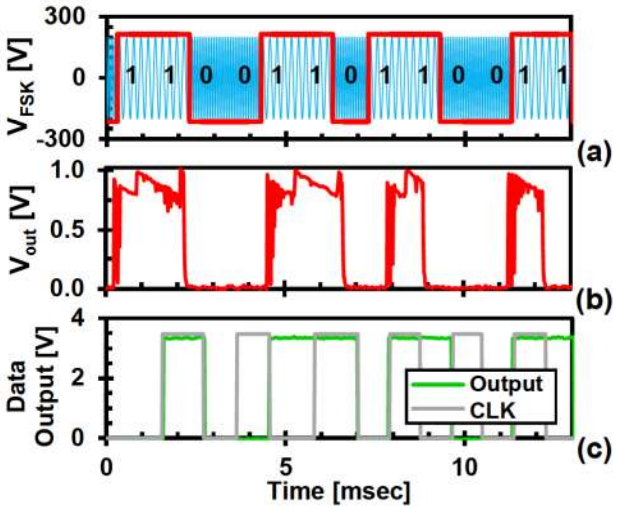

Figure 8: Waveforms at various points of Figure 2, showing successful recovery of a FSK modulated input waveform, confirmed by matching input and output bit streams.

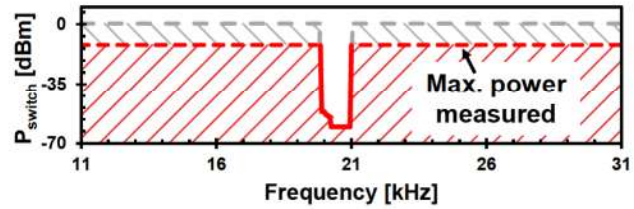

Figure 9: Frequency mask plot showing the powers needed to instigate impacting, and thus, produce an output, at various input frequencies. Although -14dBm was the maximum input power available for this measurement, rejection of out-of-channel powers higher than 0dBm are also conceivable.

Acknowledgement. This work was supported by DARPA.

REFERENCES

[1] J.R. Johler, "Propagation of the …," *Proceedings of the IRE (1962)*, vol.50, no.4, pp.404-427.
[2] Y. Lin, *et al.*, "The micromechanical …," *Hilton Head,* 2008.
[3] Y. Lin, *et al.*, "Polycide contact …," *MEMS*, 2014.
[4] R. Nathanael, *et al.*, "4-terminal relay …," *IEDM*, 2009.
[5] R.E. Mihailovich, *et al.*, "MEM relay…," *IEEE MWCL,* vol.11, no.2, pp.53-55, 2001.
[6] C. T.-C. Nguyen, "Frequency-Selective ...," *Tran. MTT*, vol. 47, no. 8, pp.1486-1503, 1999.
[7] K. Wang, *et al.*, "High-order medium frequency …," *JMEMS,* vol.8, no.4, pp.534-556, 1999.
[8] Y. Lin, *et al.*, "A metal micromechanical …," *IEDM*, 2011.
[9] "CMMR-6" Datasheet," Rev A.2, C−MAX, Aug. 2007.
[10] H.G. Barrow, *et al.*, "A Real-Time 32.768-kHz Clock Oscillator …," *IFCS*, 2012.

CONTACT

*R. Liu, liur@eecs.berkeley.edu